2016

Role of the Exopolysaccharide Alginate in Adherence to and Inflammation of Pulmonary Epithelial Cells

Brian E. Crossley
VCU

Role of the Exopolysaccharide Alginate in Adherence to and Inflammation of Pulmonary Epithelial Cells

A thesis submitted in partial fulfillment of the requirements for the degree of

Master of Science in Biology at Virginia Commonwealth University

By

Brian Edward Crossley

Bachelor of Science, Virginia Commonwealth University, 2014

Directors:

Deborah A. Lebman
Associate Professor, Microbiology & Immunology

Dennis E. Ohman
Professor and Chair, Microbiology & Immunology

Virginia Commonwealth University
Richmond, VA
August 2016

Acknowledgements

I would like to thank my major adviser Dr. Deborah Lebman for her dedication to my project throughout its course. Her consistent guidance and support has been an invaluable aspect of my education thus far. Additionally, I would like to thank Dr. Dennis Ohman for allowing me to work in his lab and providing financial support during the course of my project. Their willingness to provide expertise and technical support was crucial to the success of this thesis.

I would like to thank Scott Hirsch and Carl Rudebusch for their time spent with me in the lab during the summer months and for their contributions to my project. A special thanks goes to Dr. Richard Festa for his guidance and friendship throughout the end stages of my thesis. I would also like to thank the rest of my thesis committee: Dr. John Ryan and Dr. Jennifer Stewart for providing directional support and igniting my interest in immunological research.

I would like to thank my life partner, Grace Lee, for her love, support, and encouragement throughout our four years together. Her inspiring work ethic and academic motivation has been instrumental to my success.

Finally, I would like to thank the rest of my family and friends who have had a positive impact on my life thus far.

Table of Contents

List of Tables

List of Figures

List of Abbreviations

A549 – A549 pulmonary epithelial cells

Alg^+ – Alginate over-production

AlgT – AlgU, σ^{22}

CF – Cystic Fibrosis

CFTR – Cystic Fibrosis Transmembrane Conductance Regulator

CFU – Colony Forming Unit

DAMP – Damage Associated Molecular Pattern

LB – Luria-Bertani Broth

LPS – Lipopolysaccharide

LSM – Laser Scanning Microscope

MH-S – Murine Alveolar Macrophages

MOI – Multiplicity of Infection

NAIP – NLR family of apoptosis inhibitor proteins

NF-κB – Nuclear Factor-κB

NFDM – Non-Fat Dry Milk

NLR – Nod-like Receptor

PA – *Pseudomonas aeruginosa*

PAMP – Pathogen Associated Molecular Pattern

PRR – Pattern Recognition Receptor

T3SS – Type III Secretion System

TLR – Toll-like Receptor

WT – Wild Type

Abstract

ROLE OF THE EXOPOLYSACCHARIDE ALGINATE IN ADHERENCE TO AND INFLAMMATION OF PULMONARY EPITHELIAL CELLS

By: Brian Edward Crossley, B.S.

A thesis submitted in partial fulfillment of the requirements for the degree of Master of Science in Biology at Virginia Commonwealth University

Virginia Commonwealth University 2016

Major Director: Deborah A. Lebman, Associate Professor, Microbiology & Immunology

Pseudomonas aeruginosa (PA) infections in Cystic Fibrosis (CF) patients are not easily cleared due to the conversion from a nonmucoid to a mucoid phenotype. Alginate is an acetylated exopolysaccharide produced by mucoid PA that is responsible for increased resistance to antibiotics, host phagocytic killing, and propagating biofilm formation. Understanding the interaction between PA and host cells is critical to understanding chronic infection and inflammation in CF. In order to investigate this, we used A549 pulmonary epithelial cells and murine alveolar macrophages (MH-S) to examine host response to nonmucoid versus mucoid PA infection. Adhesion assays in A549 pulmonary epithelial cells revealed that mucoid PA mutants adhere poorly compared to their nonmucoid counterparts. Similarly, phagocytosis assays using MH-S infected with PA revealed that mucoid PA are increasingly resistant to phagocytosis. The alginate acetylation mutant FRD1175 is more susceptible to phagocytic killing than alginate^{+} FRD1. Adherence and phagocytosis of mucoid FRD1 was increased by increasing the multiplicity of infection (MOI) from 50:1 to 500:1. Furthermore,

confocal microscopy revealed that mucoid PA are inherently less inflammatory than nonmucoid strains in both A549 and MH-S. Increasing the MOI of mucoid FRD1 from 50:1 to 500:1 significantly increased caspase-1 activation in MH-S but not in A549, revealing that intensity of inflammatory signaling by epithelial cells is likely independent of increased adherence. FRD1175 infection in both A549 and MH-S revealed that alginate acetylation plays a significant role in reducing inflammasome activation. Western analysis revealed that PA does not actively induce TGF-β secretion by A549 epithelial cells. Similarly, NF-κB expression was reduced in both A549 and MH-S when infected with mucoid FRD strains, but not PA from the PAO background, suggesting FRD strains have accumulated additional mutations facilitating escape of inflammation. MH-S treated with cytochalasin D to block phagocytosis were still able to activate NF-κB signaling, suggesting NF-κB activation is adherence but not phagocytosis dependent. These data increase our understanding of the various mechanisms in which mucoid PA is able to evade host immune defenses and provides insight into potential therapies to treat PA infections.

Introduction

Host-Pathogen Interactions

Host-pathogen interactions have been extensively studied for the better part of a century. While primitive studies portrayed microorganisms playing a solely parasitic role in humans, it was later discovered that microbes can play commensal as well as mutualistic roles. When examining infection and

occurrence, early researchers learned that the ubiquitous nature of microbes did not directly translate to human infection and disease [3]. The interactions that occur between disease causing microbial organisms and hosts details a long history of virulence mechanisms and the development of a complex immune system.

Human immunity has evolved into two distinct branches: the innate and adaptive immune systems. Innate immunity seeks to provide a rapid response to danger signals from potential threats through the use of phagocytic cells such as macrophages, neutrophils, and dendritic cells. Subsequent activation of the adaptive immune system through highly complex processes of antigen presentation and clonal selection allow for incredibly diverse and specific antigenic responses. Due to the lagging initiation of the adaptive immune system, the innate immune response has been well characterized as the first, and arguably the most critical, line of defense against internalized pathogens. This process occurs through the activation of pattern recognition receptors (PRRs) via binding of unique, nonhuman, peptides often termed pathogen associated molecular patterns (PAMPs). Similarly, the innate immune system can sense damaged human ligands released while undergoing cell death denoted damage associated molecular patterns (DAMPs) [30, 32]

Epithelial Protection and Inflammation

In order to mobilize innate immune cells, pathogens must first breach the body's first layer of defense, the epithelium [24]. Epithelial cells line the body's mucosal organs such as the respiratory, gastrointestinal, and urinary tracts and

provide physical and chemical barriers to pathogens. In particular, tight junctions physically block entry whereas lysozymes and β-defensins serve as antimicrobial peptides naturally secreted by mucosal epithelial cells [12, 23]. Similarly, mechanical features of these cells organize to form mucociliary elevators which serve to physically expel bacteria from the lungs [6]. In the event that these initial defenses fail, microbial entry and subsequent colonization may occur and cause pathogenesis, thus activating innate, tissue-resident phagocytic cells and causing the release of proinflammatory mediators. The onset of inflammation occurs in order to recruit additional innate phagocytic cells to the site of infection by increasing vascular leakage and diapedesis [24]. The process of inflammation is highly controlled and is regulated in order to quickly resolve and return to a homeostatic state; however, when infections are unable to be cleared, chronic inflammation may result in damage to the host. Although inflammation has protective and beneficial effects in acute infections, its role in chronic infections is not fully understood [15].

Pseudomonas *aeruginosa*

Pseudomonas aeruginosa (PA) is a ubiquitous environmental bacterium that exists in extremely diverse, moist environments. Clinically, it is an opportunistic pathogen that typically infects immunocompromised or wounded patients due to a variety of reasons, such as burns, surgery, chronic obstructive pulmonary disease, and cystic fibrosis. The wild type PA strain PAO1 was isolated from a wound in 1954, and is now the most common reference strain

when examining PA [26]. Healthy individuals exposed to PA clear the bacteria easily, without inducing noticeable inflammation. Several hypotheses have emerged addressing how PA are increasingly adherent to CF epithelial cells, such as ineffective mucociliary clearance of bacteria from hyperabsorption of water [6]; however the exact mechanisms are not completely understood. Early PA colonizing the pulmonary epithelium typically exist as non-mucoid colonies. However, as infection persists and host defenses mobilize, the bacteria must undergo phenotypic changes in order to survive in the harsh environment. The conversion from non-mucoid to mucoid colonization indicates significantly poorer prognosis for CF patients. This form of adaptation is due to a mutation in the negative translational regulator, *mucA*, of the alginate biosynthetic operon. After mutational deactivation of the anti-sigma factor *mucA*, the sigma factor AlgT (also known as σ^{22}/ AlgU) interacts with the translational regulator AlgR, thus inducing expression of the *algD* operon and initiating alginate biosynthesis [11, 36]. Alginate is an acetylated exopolysaccharide formed from D-mannuronic acid and L-guluronic acid produced that confers resistance to antibiotics, host phagocytic killing, and increased biofilm production [45] (Figure 1). The PA strain FRD1 is a mucoid clinical isolate obtained from a sputum sample of a chronically infected CF patient, which constitutively expresses alginate due to the mutational deactivation of *mucA*. Utilization of FRD1 provides insight to characterize the genomic mutations responsible for increased persistence during infection. Previously constructed mutants of both PAO1 and FRD1 provide opportunities to further identify how the structure and expression of alginate protect PA from host

immune defenses. PDO300, a PAO1 mutant, has a constructed *mucA* mutation, which allows for the overproduction of alginate; while FRD1131 is a FRD1 mutant with the transposon *algD*:: Tn*501-33*, inserted just before the first gene, *algD,* within the alginate promoter; therefore, blocking synthesis of alginate. Similarly, FRD1175 and FRD462 are FRD1 mutants with acetylation and epimerization defects, respectively. Alginate acetylation occurs at the C2-C3 hydroxyl substituents on mannuronic acid residues, and confers resistance to opsonic phagocytosis through the blockade of receptors capable of binding complement opsonins [38]. FRD1175 is unable to O-acetylate alginate due to a constructed mutation on *algF*, which is one of three products within the alginate synthesis operon required for acetylation, alongside *algI and algJ* [13, 38]. Alginate epimerization is mediated by AlgG, a C5 epimerase and occurs through subsequent conversion of 20-40% of mannuronate residues to form linkages between alternating D-mannuronate and L-guluronate molecules [44]. These epimerase linkages give rise to increasingly viscous and gelation properties of alginate, further increasing PA ability to evade host defenses [44]. FRD426 has a constructed mutation in AlgG, which prevents C-5 epimerase from converting mannuronate residues to linkages between mannuronate and guluronate. By examining host interactions with FRD1175 and FRD426, we can evaluate the effects of the structure of alginate, beyond simply its expression. PA strains used in this study are outlined in Table 1.

Virulence factor expression varies greatly between acute and chronic PA infections. Acute PA infections invoke a variety of inflammatory molecules in

order to actively establish infection, whereas chronic PA infections rely heavily on the down regulation of these same virulence factors [14]. Acute infections are facilitated via adhesion molecules such as flagella, type 4 pili, and lipopolysaccharide (LPS). Once PA have successfully attached to host epithelium, activation of the type 3-secretion system (T3SS) further exacerbates cytotoxic effects on the host through the injection of effector molecules ExoU, ExoS, ExoT, ExoY [14, 20]. Similarly, a multitude of proteases secreted by PA enable colonization through the disruption of tight junctions and degradation of host lung proteins [14, 25].

During the course of chronic infection, PA undergo a variety of adaptive mutations that increase the likelihood of survival in the presence of host immune cells. Most notably, the ability of chronic PA to undergo a conversion from non-mucoid to mucoid phenotype allows for the cultivation of antibiotic resistant biofilms. In doing so, it is common for mucoid PA to down regulate many virulence genes such as components of the T3SS, LPS side chains, and flagellin, the main structural component of flagella. This inverse relationship between expression of flagella and T3SS is mediated via AlgT. Flagella are potent activators of host immunity through recognition and binding to TLR5, causing increased inflammatory signaling and mobilization of innate immune cells [14, 33]. Similarly, T3SS effector molecules enhance host recognition of PA through NAIP (NLR family of apoptosis inhibitor proteins) sensors and cause subsequent formation of the inflammasome complex.

Cystic Fibrosis

Cystic Fibrosis (CF) is an autosomal recessive disorder resulting from an accumulation of mutations in the gene regulating the Cystic Fibrosis Conductance Transmembrane Regulator (CFTR). These mutations cause chloride ion transporters to become defective in epithelial cells, leading to increased secretion of chloride in sweat, hyperabsorption of sodium, infertility, and chronic pulmonary disease [19, 39, 43]. While CF typically affects organs throughout the body, the major cause of morbidity and mortality in affected patients is deterioration of lung function due to chronic inflammation, remodeling of epithelial cells, decreased expiration rates, and chronic infection from PA [9, 34]. Furthermore, the pathophysiology of CTFR defects in epithelial cells extends beyond chloride ion transport. Notably, this mutation has been shown to affect a multitude of other processes such as vesicle trafficking and increased expression of a variety of cytokines which modulate inflammation, such as IL-8 and IL-10 [2, 8]. Despite this, it has been hypothesized that lungs in infants and young CF patients are inherently uninflamed until actual infections occur [1], reinforcing the hypothesis that infection precedes inflammation. Increased neutrophil presence in CF patients compared to normal patients has also been described to exacerbate the inflammatory response, possibly due to increased release of IL-8 by CF epithelial cells [1, 8]. It has been suggested that excessive influx of neutrophils into the airway is an ineffective immune response to PA infections within CF patients.

Inflammatory Response and Activation of the Caspase-1 Inflammasome in the CF lung.

The initial immune response to infections within the lung involves pulmonary epithelial cells, neutrophils, and alveolar macrophages, which in turn secrete a variety of cytokines controlling the inflammatory response [10]. These cytokines act on a variety of receptors and cell transcription factors, such as Nuclear Factor-κB (NF-κB). Ligand binding to TLRs activates the NF-κB signaling canonical signaling pathway, which triggers subsequent activation of a wide range of downstream kinases that in turn lead to cell survival, proliferation, and cytokine production. [27]. The effects of proinflammatory cytokines such as IL-1β, which are readily secreted by alveolar macrophages and epithelial cells, can be reversed by anti-inflammatory cytokines, such as TGF-β [31].

Upon recognition of foreign ligands via PAMPs, mobilized innate immune cells boast a variety of defenses. Most notably, monocytes and macrophages secrete proinflammatory mediators, which exhibit one of two fates: activation of the inflammasome, or encouragement of apoptotic cell death pathways [7, 29]. The caspase-1 inflammasome exists as a multimeric protein complex composed of a variety of PRRs including the NLR family (Nod-like receptor), NAIP sensors, and pro-caspase [16]. The sensing of different bacterial ligands triggers the recruitment and formation of different inflammasome proteins. With respect to bacterial infections, it has been determined that the NLRC4 inflammasome is stimulated by bacterial flagellin and components of the T3SS [16, 33]. These bacterial products are initially sensed by NAIP receptors before allowing downstream NLRC4 to directly recruit caspase-1 activators via its CARD domain, which in turn drives antimicrobial responses [42]. Activated caspase-1 results in

the cleavage of pro-IL-1β and subsequent recruitment of neutrophils to amplify bacterial clearance [33, 42].

Specific Aims of This Project

Understanding the interaction between PA and host cells is critical to fully understanding the pathogenesis of CF. In order to examine these interactions, we sought to determine how the alteration in PA accompanying chronic infection contributes to the inflammasome and the surrounding environment. Specifically, we examined how host response cytokine production is affected by various mucoid transformations in addition to alterations in cell signaling pathways. In addition, we determined how mucoid conversion and alginate expression alters the interaction between epithelial cells and PA. Although studies have shown that adaptations in PA clearly inhibit innate immunity, the mechanisms within the inflammasome due to these changes are poorly understood. By further understanding the host-pathogen interactions that alter the inflammatory response, it could shed light in the treatment of chronic infection and lead to a better understanding of potential therapies for cystic fibrosis patients.

Materials & Methods

A549 Culture

A549 epithelial cells from a human lung adenocarcinoma were cultured in complete F12-HAMS (Hyclone) supplemented with 10% FBS (Atlanta Biologicals), 1% penicillin and streptomycin, and 1% L-glutamine. Cells were monitored for confluency and passed every 3-4 days. Fresh cultures stored were

stored in a -80^{o}C freezer were thawed every 3-4 months. Prior to use, cells were counted using a hemocytometer or Bio-Rad Automated Cell Counter before plating.

Macrophage Culture

Murine Alveolar Macrophages (MH-S) were cultured in complete RPMI (Gibco) supplemented with 10% FBS (Atlanta Biologicals), 1% penicillin and streptomycin, and 1% L-glutamine. Cells were monitored for confluency and passed every 3-4 days. Fresh cultures were stored in a -80^{o}C freezer were thawed every 3-4 months. Prior to use, cells were counted using a hemocytometer or Bio-Rad Automated Cell Counter before plating.

***Pseudomonas aeruginosa* Growth Conditions**

All PA strains were newly streaked from frozen stocks and grown on solid Luria-Bertani (LB) agar plates 3 days prior to use. Following initial growth on agar plates, single colonies were isolated and diluted in LB liquid broth at 37^{o}C with shaking overnight.

***Pseudomonas aeruginosa* Strains**

Strains are outlined in Table 1. FRD1 is a clinical isolate from a sputum from a CF patient. FRD1 actively produces alginate due to a *mucA* mutation which fails to prevent σ^{22} from binding to the promoter and initiating transcription. FRD1131 is a FRD1 mutant with the transposon, *algD*:: Tn*501-33*, inserted just before the first gene, *algD,* within the alginate promoter; therefore, blocking synthesis of alginate. FRD462 is a FRD1 *algG* mutant with a defective C5

epimerase rendering it unable to form complete alginate, instead only forming D-mannuronate. FRD1175 is a FRD1 *algF* mutant, which is unable to O-acetylate D-mannuronate. PAO1 is the wild type (WT) from a clinical burn wound. PDO300 is a PAO1 mutant with a constructed *mucA22* mutation, causing it to readily produce alginate.

Epithelial Cell Adherence Assay

$2x10^5$ A549 epithelial cells were plated in complete F12-HAMS (Hyclone) in 12-well plates 24 hours before infection. Cells were washed once with warm serum free/ antibiotic free F12-HAMS 6 hours prior to infection. Overnight cultures of *Pseudomonas aeruginosa* were diluted 1:50 and grown for 4 hours until mid-log phase (0.8 OD/600nm). A549 cells were infected at a MOI of 50:1 or 500:1 and incubated at 37^{o}C, 5% CO_2 for 1 hour. A549 cells were washed three times with cold PBS and then lysed with 0.1% Triton (Sigma). Cell lysate was then collected by scraping and underwent 1:10 serial dilutions before plating on LB agar plates. Plates were incubated at 37^{o}C overnight. Colonies were counted the following day to determine Colony Forming Units (CFU).

Phagocytosis Assay with Gentamicin Protection

$2x10^5$ murine alveolar macrophages (MH-S) were plated in complete RPMI (Gibco) in 12-well plates 24 hours before infection. Cells were washed once with warm serum free/ antibiotic free RPMI 6 hours prior to infection. Overnight cultures of *Pseudomonas aeruginosa* were diluted 1:50 and grown for 4 hours to mid-log phase (0.8 OD/600nm). MH-S cells were infected at a MOI of

50:1 or 500:1 and incubated at 37^{o}C, 5% CO_2 for 30 minutes. MH-S cells were washed twice with warm RPMI, and then gentamicin was added to each well at a concentration of 2 mg/ml and then re-incubated at 37^{o}C, 5% CO_2 for 30 minutes. MH-S cells were washed twice with cold PBS and then lysed with 0.25% SDS. Cell lysate was then collected by scraping and underwent 1:10 serial dilutions before plating on LB agar plates. Plates were incubated at 37^{o}C overnight. Colonies were counted the following day to determine Colony Forming Units (CFU).

Fluorescent Microscopy- Caspase-1

4x10^{5} A549 or MH-S cells were plated in complete cell line media in 27mm Glass Base Dishes (Thermo Sci) 24 hours prior to infection. Cells were washed once with serum free/ antibiotic free media 6 hours prior to infection. Overnight cultures of *Pseudomonas aeruginosa* were diluted 1:50 and grown for 4 hours until mid-log phase (0.8 OD/600nm). A549 or MH-S cells were infected at a MOI of 50:1 or 500:1 and incubated at 37^{o}C, 5% CO_2 for 1 hour. A549 or MH-S cells were washed twice with cold PBS and replaced with 300 µl warm cell line media. FLICA reagent was prepared according to the manufacturer's instructions (Invitrogen). 10 µl FLICA reagent was added per 300 µl cell culture and then incubated at 37^{o}C, 5% CO_2 for 1 hour. A549 and MH-S cells were washed once with warm cell line media and then incubated with 1 µM Hoechst 33342 Nuclear Stain (Invitrogen) at 37^{o}C, 5% CO_2 for 10 minutes. A549 and MH-S cells were fixed with 4% paraformaldehyde (Affymetrix) in PBS for 15 minutes.

Paraformaldehyde was removed and replaced with cold PBS prior to viewing on a Zeiss LSM 710 at 40x or 63x magnification.

Western Blotting Analysis

$2x10^5$ A549 or MH-S cells were plated in complete cell line media in 6 well plates 24 hours prior to infection. Overnight cultures of *Pseudomonas aeruginosa* were diluted 1:50 and grown for 4 hours to mid-log phase (0.8 OD/600nm). A549 or MH-S cells were infected at a MOI of 50:1 or 500:1 and incubated at 37^{o}C, 5% CO_2 for 1 hour. A549 or MH-S cells were washed twice with cold PBS. A549 or MH-S cells were lysed with 70 µl RIPA buffer (Thermo Sci) containing 5 µl protease inhibitor (Thermo Sci), 5 µl phosphatase inhibitor (Thermo Sci), and 5 µl PMSF (Thermo Sci). Cell lysate was scraped and harvested before being centrifuged at 4^{o}C for 15 minutes. Supernatants were collected and stored at -80^{o}C for further analysis. Protein concentrations were determined using a Bradford Protein Assay. 20 µg of protein was separated on an 8%, 10% or 12% polyacrylamide gel in Tris-Glycine buffer at 175 volts for 70 minutes. Proteins were then transferred onto PVDF membranes using a Semidry Transfer cell in Towbin (Tris-Glycine-SDS) buffer at 25 volts for 30 minutes. The membranes were allowed to dry for 15 minutes before being blocked in 5% Nonfat Dry Milk (NFDM) in TBS containing 0.01% Tween for 45 minutes. Various rabbit primary antibodies (Cell Signaling) were diluted 1:1000 in 5% NFDM in TBS/Tween and were allowed to attach at 4^{o}C with gentle shaking overnight. The membranes were washed three times with TBS/Tween for 10 minutes each and then labeled with an anti-rabbit secondary antibody (Cell Signaling) diluted 1:10000 in 2.5%

NFDM in TBS/Tween. Membranes were then washed four times in TBS/Tween for 15 minutes each. Perkin Elmer chemiluminescence substrates were added to membranes for one minute before being exposed to x-ray film. When stripping in order to tag membranes with various primary antibodies, stripping buffer (2-beta mercaptoethanol, 10% SDS, Tris 6.8M) was added to membranes at 55^{o}C with rotation for 30 minutes. Membranes were then washed 5 times in TBS/Tween for 5 minutes each before being re-blocked.

Results

Effects of mucoidy on lung epithelial adherence of PA.

The current dogma of activating immunity begins with adherence and subsequent breachment of the epithelium, where pathogens are encountered by innate immune cells [24]. In cystic fibrosis, opportunistic PA successfully colonizes the lung epithelium in a non-mucoid state. However, due to increasingly harsh environmental conditions, mutations give rise to mucoid colonies, characterized by the production of exopolysaccharide alginate. In order to address mucoidy effects on epithelial adherence, A549 lung epithelial cells were infected at a multiplicity of infection (MOI) of 50:1 or 500:1 for 1 hour. The data showed that mucoid PA were unable to adhere to A549 epithelial cells as well as non-mucoid strains. After increasing the MOI of FRD1 from 50:1 to 500:1, in order to achieve equal adherence to a non-mucoid strain, FRD1131, the number of FRD1 adhering to A549 epithelial cells was significantly increased (Figure 2). These data suggest that increasing the multiplicity of infection of PA can increase overall adherence.

Mucoidy effects on phagocytosis of PA by alveolar macrophages.

In cystic fibrosis, research has shown that the colonization of mucoid PA is not easily cleared by host immune cells [45]. Because alveolar macrophages serve as one of the primary host defenses of lung infections, we investigated the effects of mucoidy on phagocytosis. Murine alveolar macrophages were infected with various PA strains at an MOI of 50:1 or 500:1 for 30 minutes. Our data suggests that mucoid PA strains are phagocytosed significantly less than non-mucoid strains. After increasing the MOI of FRD1 from 50:1 to 500:1, the number of FRD1 being phagocytosed was significantly increased. These data also suggest that alginate acetylation, but not alginate epimerization, decreases the ability of alveolar macrophages to phagocytose mucoid PA (Figure 3). These data further support previous studies detailing the protective nature of substituted acetyl groups by blocking access of opsonins from attaching to PA surface [38].

Mucoidy effects on inflammasome activation in A549 epithelial cells and murine alveolar macrophages.

Inflammasome activation plays a critical role in the maturation of pro-inflammatory mediators in order to amplify bacterial clearance [33, 42]. In order to assess the effects of mucoidy on inflammasome activation, we quantified total caspase-1 activation following infection with various PA strains in A549 epithelial cells and murine alveolar macrophages for 1 hour via confocal microscopy. Our data suggests that mucoid PA significantly decreases caspase-1 signaling compared to non-mucoid strains in A549 epithelial cells (Figure 4) and alveolar

macrophages (Figure 5). These data suggest that mucoid PA are inherently less inflammatory than nonmucoid strains.

Increasing multiplicity of infection in mucoid PA increased caspase-1 activation in murine alveolar macrophages, but not in A549 epithelial cells.

Our previous data showed that the amount of mucoid PA adhering to lung epithelial cells and alveolar macrophages was significantly less than the amount of non-mucoid colonies adhering. In order to determine if increased adherence led to increased caspase-1 activation, we increased the multiplicity of infection of FRD1 from 50:1 to 500:1, and then quantified caspase-1 activation following infection with various PA strains for 1 hour via confocal microscopy. These data suggest that bacterial adherence does not translate directly to caspase-1 activation in A549 epithelial cells (Figure 6). In contrast, increased MOI of FRD1 significantly increased the amount of caspase-1 activation in murine alveolar macrophages (Figure 7).

***Alginate acetylation, but not alginate* epimerization, decreased caspase-1 activation in A549 epithelial cells and murine alveolar macrophages.**

Since our data above suggested that macrophages exhibited improved phagocytosis of non-acetylated, mucoid PA, we examined the effects of alginate acetylation and epimerization on activation of caspase-1 in A459 epithelial cells and murine alveolar macrophages via confocal microscopy. These data suggest that non-acetylated, mucoid bacteria activate caspase-1 significantly more than acetylated, mucoid bacteria in A549 epithelial cells (Figure 8) and murine

alveolar macrophages (Figure 9). Alginate epimerization did not play a role in caspase-1 activation.

PA did not induce TGF-β secretion in A549 epithelial cells.

TGF-β acts as an anti-inflammatory cytokine, and is primarily produced in the lungs by alveolar macrophages and epithelial cells [31]. In order to assess if mucoidy was responsible for inducing anti-inflammatory signaling in epithelial cells, western analysis for phosphorylated SMAD2/3 was performed following infection with various PA strains at an MOI of 50:1 or 500:1 for 1 hour. These data suggest that infection with PA does not induce TGFβ secretion in A549 epithelial cells, regardless of alginate expression (Figure 10).

Analyzing NF-κB expression in A549 epithelial cells and murine alveolar macrophages after infection with PA.

Our data above suggested that mucoid strains of PA were generally reduced in the amount of caspase-1 activation with both A549 epithelial cells and murine alveolar macrophages. In order to further assess the ability of mucoid and nonmucoid PA to induce inflammation, western analysis for phosphorylated NF-κB (p65) was performed following infection with various PA strains at an MOI of 50:1 or 500:1 for 1 hour in A549 epithelial cells. Phosphorylation of p65 was only slightly elevated in PA strains that were of the PAO1 background, compared to the FRD strains in A549 epithelial cells. These data also suggest that mucoidy and MOI may play larger roles in activating NF-κB in the FRD strains (Figure 11). Similarly, phosphorylation of p65 was assessed in resting and cytochalasin D treated murine alveolar macrophages following infection with various PA strains

at an MOI of 50:1 or 500:1 for 1 hour. Phosphorylated p65 was slightly suppressed in FRD1 and FRD462 infected alveolar macrophages, compared to the other PA strains (Figure 12). Cytochalasin D treated alveolar macrophages did not seem to inhibit p65 phosphorylation, suggesting that phagocytosis of PA was not necessary in order to activate inflammatory signaling (Figure 12).

Analyzing Caspase-1 cleavage in A549 epithelial cells after infection with PA.

Our data above collected by confocal microscopy suggested that mucoid PA decreased caspase-1 activation in A549 epithelial cells. In order to confirm this finding, western analysis for cleaved caspase (p20) was performed following infection with various PA strains at an MOI of 50:1 or 500:1 for 1 hour. Levels of p20 were decreased in Alg^+ FRD1 compared to the other FRD strains. These data also suggested that increasing the MOI of FRD1 from 50:1 to 500:1 increased the amount of cleaved caspase, differing slightly from our previous results in Figure 6 (Figure 13).

DISCUSSION

Chronic PA infections have are a major cause of morbidity and mortality in CF patients [18, 21]. The inherent difficulties of CF patients to clear excessive mucus, in addition to the adaptive abilities of PA allow for persistent infections; this is also partially due to improved resistance to many antibiotics [18]. A major pathoadaptive change in PA within the CF lung involves the transition from a non-mucoid to the mucoid phenotype, often characterized by the deactivation mutation within the translational regulator encoded by *mucA* [45]. This mutation

results in excessive production of the exopolysaccharide alginate, which confers resistance to many host defense factors as well as aiding biofilm formation and protection [28]. Our lab has previously characterized the role of alginate in the inhibition of macrophage phagocytosis [40], but the role of alginate in adherence and inflammasome activation in epithelial cells remained unclear. In order to address these issues, we expanded our studies to include A549 alveolar epithelial cells based on the paradigm of innate activation of inflammation and implications in previous studies [18]. Parallel studies with A549 alveolar epithelial cells and murine alveolar macrophages infected with various PA strains were used in order to characterize the role of alginate in adherence and activation of inflammation in pulmonary epithelial cells and macrophages.

In this study, we began to unravel questions regarding the ability of PA to escape host immune responses. While previous studies have often compared various PA strains at the same MOI, we showed that by increasing the MOI of a mucoid strain (FRD1), similar adherence and phagocytosis could be achieved to a nonmucoid mutant of the same strain (FRD1131). By eliminating the effect of reduced adherence, we could more effectively compare the amount of inflammatory signaling between nonmucoid and mucoid PA strains. Our data revealed that caspase-1 signaling in A549 epithelial cells did not significantly increase when infected with FRD1 at an MOI of 50:1 or 500:1. This result suggested that the CF clinical isolate, FRD1, is inherently less inflammatory than its nonmucoid mutant. This suggests that the inverse relationship between alginate and T3SS expression plays a significant role in dampening host

immunity [41]. We hypothesized that alginate expression in FRD1 may result in a significant physical barrier thick enough to block entry of the T3SS needle into host cytoplasm. Similarly, the repression of T3SS in clinical isolates has been shown to reduce virulence, and allow PA the ability to escape inflammation [22, 46]. While the exact mechanism is unknown, the maturation of chronic PA from the accumulation of mutations may confer increased resistance to host immunity through repression of T3SS rather than relying on T3SS effector molecules ExoT, ExoU, and ExoS to block the maturation of caspase-1 [17]. Similarly, the repression of flagellum expression has shown to dampen host immunity. Previous reports suggest that loss of flagellar motility, independent of flagellar expression, reduces IL-1β secretion and caspase-1 activation in macrophages Through the loss of flagellar motility, decreased cell surface interactions with host cell receptors may play a role in escaping immune cell function [37]. This conclusion aligns with results of this study, suggesting that decreased adhesion serves as an important mechanism for bacterial persistence in the CF lung. In murine alveolar macrophages, slight increases in caspase-1 signaling were seen when increasing the MOI of FRD1 from 50:1 to 500:1, but remained significantly less than that of Alg^- FRD1131. This result may be due to increased phagocytosis and internalization of FRD1 bacteria, thus leading to the increased activation of caspase-1.

Alginate in PA exists as an ester linked polymer of D-mannuronate and L-guluronate, which confers formation of many O-acetyl groups on the C-2 and C-3 acid residues of mannuronic acid, thus providing increased virulence [38]. *O*-

acetylation of alginate has been shown to contribute to biofilm formation and its structural integrity [12]. In this study, we evaluated the effects of alginate structure in activating the inflammasome. Our data did not reveal any significant increases in non-acetylated PA (FRD1175) adhesion to A549 epithelial cells, but did show increased caspase-1 activation in both A549 epithelial cells and murine alveolar macrophages. A previous study revealed how alginate hydroxyl linkages dampen opsonic phagocytosis through the blockade of unsubstituted hydroxyl residues capable of binding complement proteins to the bacterial surface [38]. This could help explain the increased caspase-1 activation seen in both A549 and MH-S cells when infected with non-acetylated, mucoid PA. Western blot analysis of phosphorylated NF-κB showed slightly increased activity in both cell lines when infected with non-mucoid or non-acetylated FRD strains. This result suggests the ability to interact with aggregated host cell receptors is necessary to activate NF-κB. Previous reports have suggested that alginate expression and presence is capable of altering host responses not seen in motile PA strains, in addition to the blockade of TLR-2,-4, and-5, rendering airway epithelial cells unable to activate NF-κB [5] [35]. Similarly, the increased activation of NF-κB seen in non-acetylated FRD1175 alginate may be due to the loss of alginate structural integrity, thus allowing host TLRs to induce downstream signaling. The treatment of MH-S macrophages with 10 μM Cytochalasin D did not affect the activity of phosphorylated NF-κB, revealing that internalization of TLRs was not necessary to initiate downstream signaling.

In summary, these data increased our understanding of the various mechanisms by which mucoid PA is able to evade host immune defenses. The ability of PA to escape inflammation in A549 alveolar epithelial cells is dependent on the strain background, alginate expression, and alginate structure. These data reveal that further investigation of alginate is needed, and supports that targeting alginate acetylation as a valid therapeutic target.

Tables & Figures

Table 1: Description of Bacterial Strains

PA Strain	Gentoype	Mucoid	Phenotype
FRD1	*mucA22* Alg+ LPS-O-	+	Poly Mannuronate/Guluronate, Acetyl+
FRD1131	FRD1*algD*::Tn*501-33* Alg-	-	
FRD462	FRD1 *algG4*	+	Poly Mannuronate
FRD1175	FRD1 *algF2*	+	Poly Mannuronate/Guluronate, Acetyl-
PAO1	WT Alg- LPS-O+	-	
PDO300	PAO1*mucA22* Alg+	+	Poly Mannuronate/Guluronate, Acetyl+

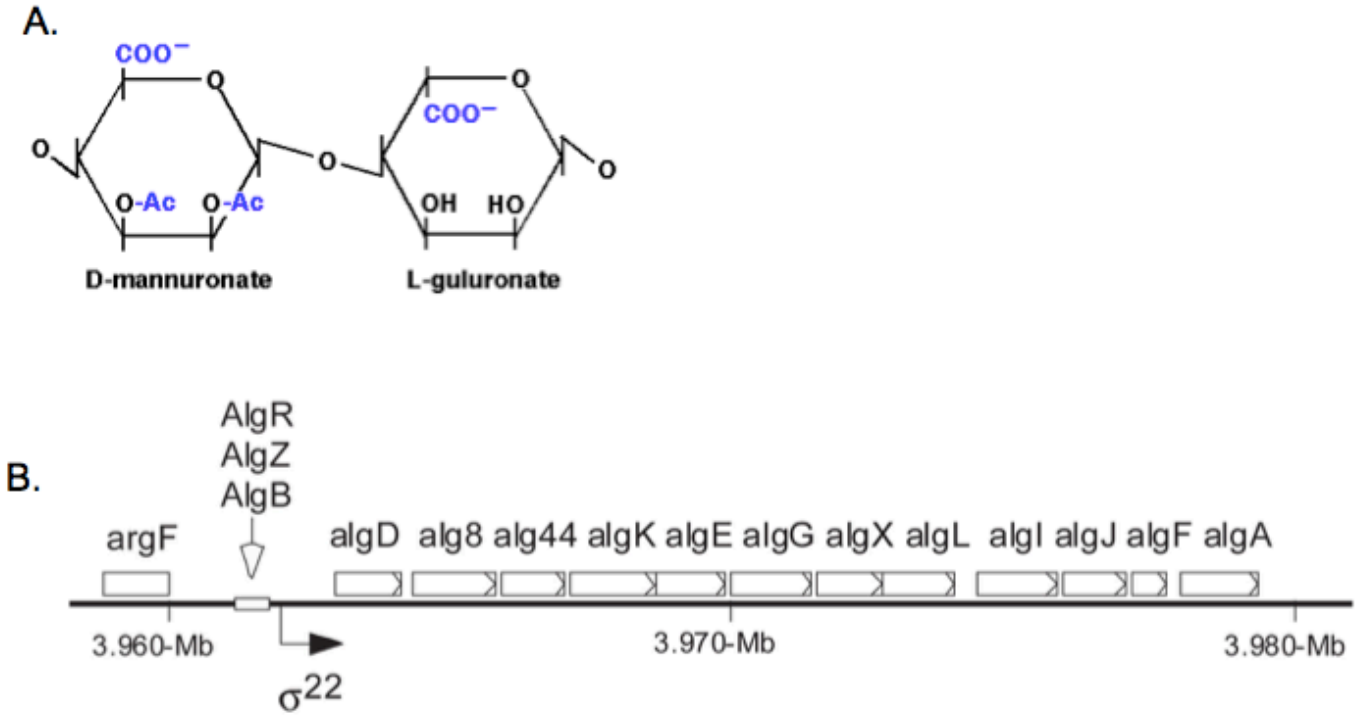

Figure 1: A. Structure of Alginate. B. Alginate Biosynthetic Operon [4]

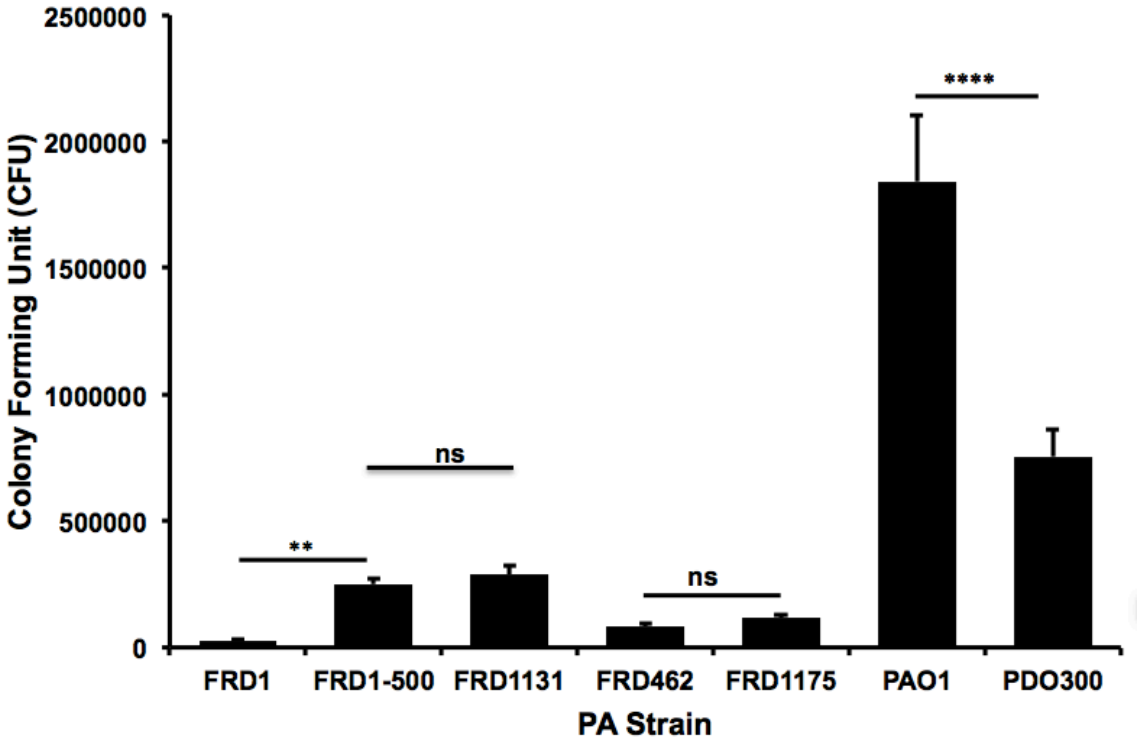

Figure 2: Adherence of *P. aeruginosa* to A549 Epithelial Cells. A549 cells were plated at $2x10^5$ in complete F12-HAMS 24 hours prior to infection. Overnight cultures of *Pseudomonas aeruginosa* were diluted 1:50 and grown for 4 hours until mid-log phase (0.8 OD/600nm). A549 cells were infected at a MOI of 50:1 or 500:1 and incubated at 37^{o}C, 5% CO_2 for 1 hour. Cell lysate was collected plated on LB agar plates. Plates were stored at 37^{o}C overnight. Colonies were counted the following day to determine Colony Forming Units (CFU). Statistical analysis was performed by ANOVA followed by Tukey's test. *P<0.05, **P<0.01, ***P<0.001, ****P<0.0001, ns: not significant.

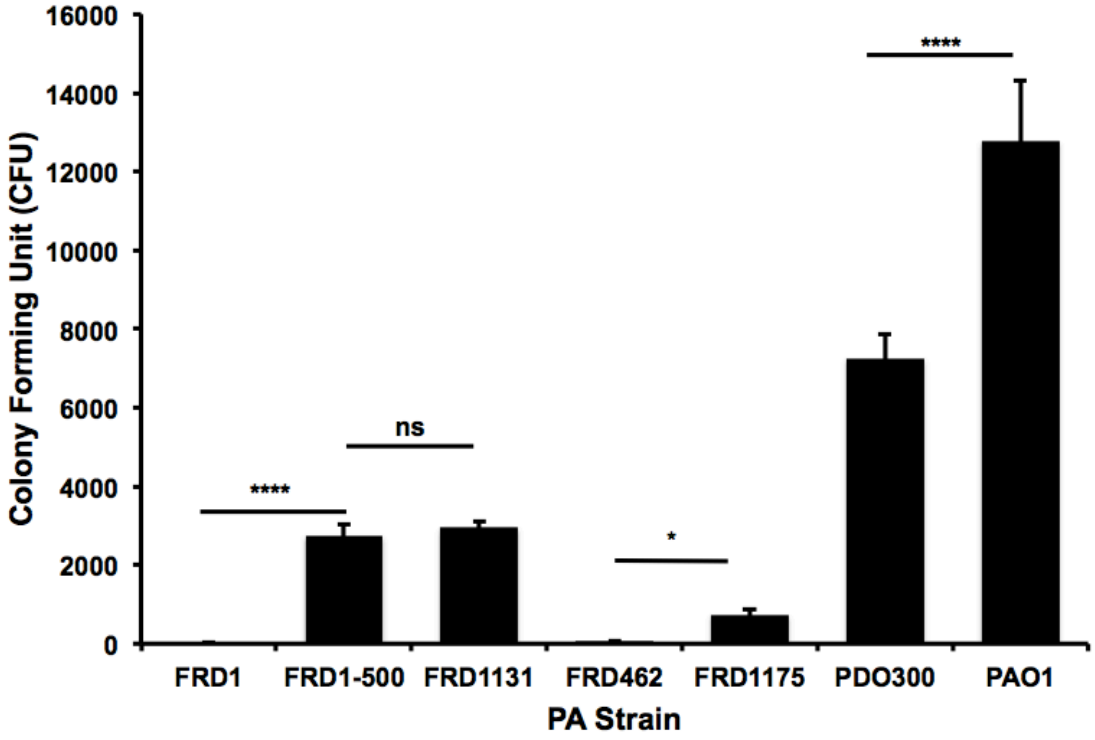

Figure 3: Phagocytosis of *P. aeruginosa* by Murine Alveolar Macrophages. MH-S cells were plated at $2x10^5$ in complete RPMI 24 hours prior to infection. Overnight cultures of *Pseudomonas aeruginosa* were diluted 1:50 and grown for 4 hours until mid-log phase (0.8 OD/600nm). MH-S cells were infected at a MOI of 50:1 or 500:1 and incubated at 37°C, 5% CO_2 for 30 minutes. Gentamicin was added to each well at a concentration of 2mg/ ml and then re-incubated at 37°C, 5% CO_2 for 30 minutes. Cell lysate was collected plated on LB agar plates. Plates were stored at 37°C overnight. Colonies were counted the following day to determine Colony Forming Units (CFU). Statistical analysis was performed by ANOVA followed by Tukey's test. *P<0.05, **P<0.01, ***P<0.001, ****P<0.0001, ns: not significant.

A.

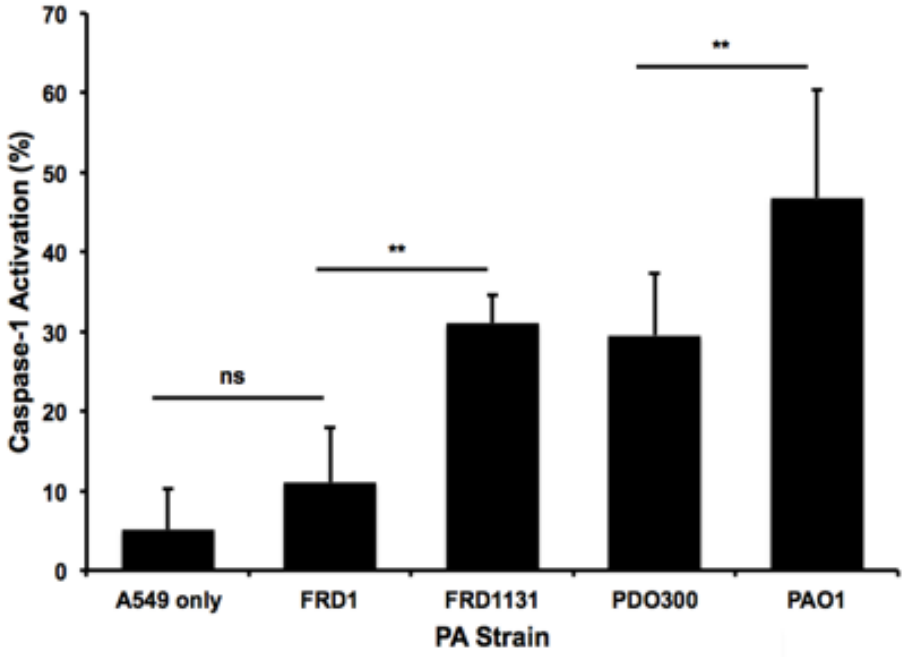
Caspase-1 Activation (%)
70
60
50
40
30
20
10
0
ns
**
**
A549 only
FRD1
FRD1131
PDO300
PAO1
PA Strain

B.

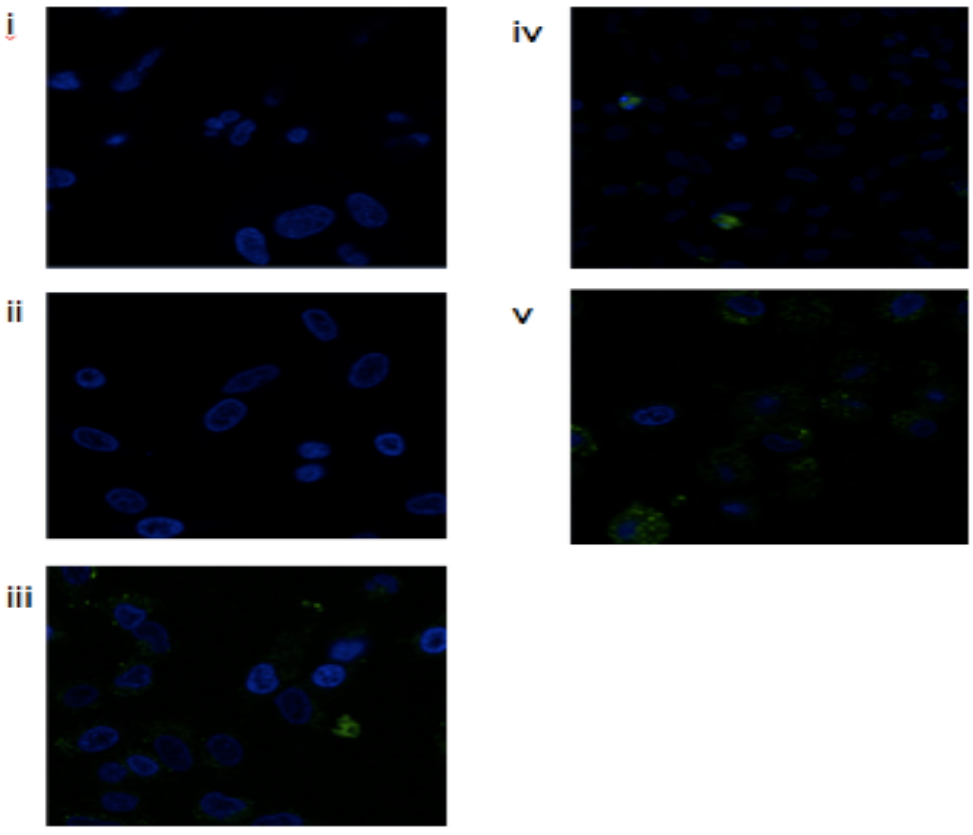
i
ii
iii
iv
v

Figure 4: Caspase-1 Activation in A549 epithelial cells post infection with *P. aeruginosa.* $4x10^5$ A549 cells were plated in complete F12-HAMS in 27mm Glass Base Dishes 24 hours prior to infection. Complete F-12 HAMS was washed once with serum free/ antibiotic free media 6 hours prior to infection. Overnight cultures of *Pseudomonas aeruginosa* were diluted 1:50 and grown for 4 hours until mid-log phase (0.8 OD/600nm). A549 cells were infected at a MOI of 50 and incubated at 37^oC, 5% CO_2 for 1 hour. Caspase probe (Invitrogen) was attached for 1 hour before fixing cells and viewing on a Zeiss Laser Scanning Microscope (LSM710). (A) Quantification of percentage of caspase-1^+ cells following infection with indicated PA strain. (B) A549 cells were uninfected (i), infected with FRD1 (ii), FRD1131 (iii), PDO300 (iv), or WT PAO1 (v). Cells were stained for cleaved caspase-1 (FAM-FLICA) and DNA (Hoechst 33342). Images were taken at 63x magnification. Minimum of 100 cells were counted for quantification. Data are a sum of triplicate experiments. Statistical analysis was performed by ANOVA followed by Tukey's test. *P<0.05, **P<0.01, ***P<0.001, ****P<0.0001, ns: not significant.

A.

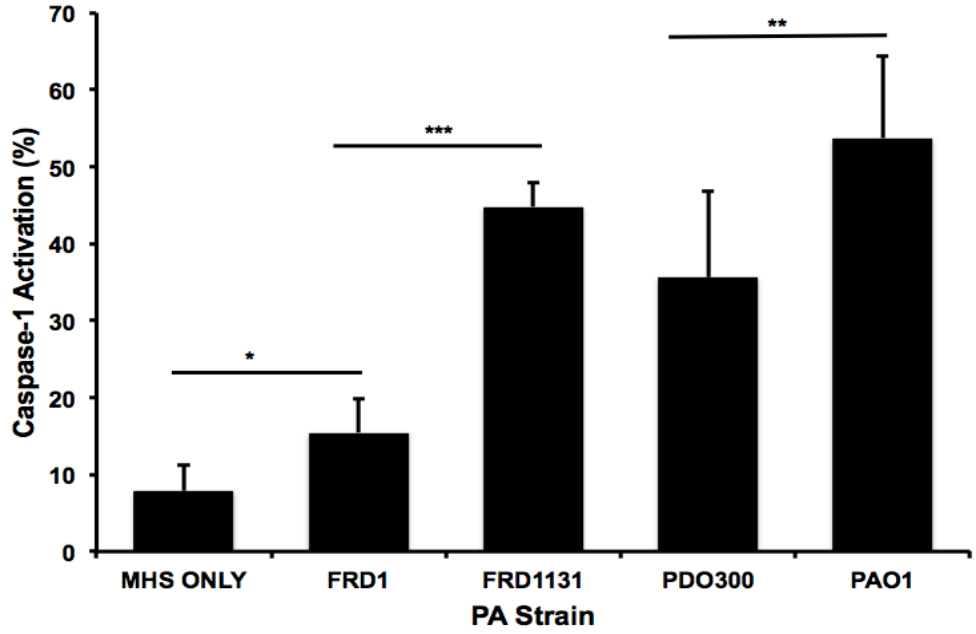
Caspase-1 Activation (%)
70
60
50
40
30
20
10
0
*
***
**
MHS ONLY
FRD1
FRD1131
PDO300
PAO1
PA Strain

B.

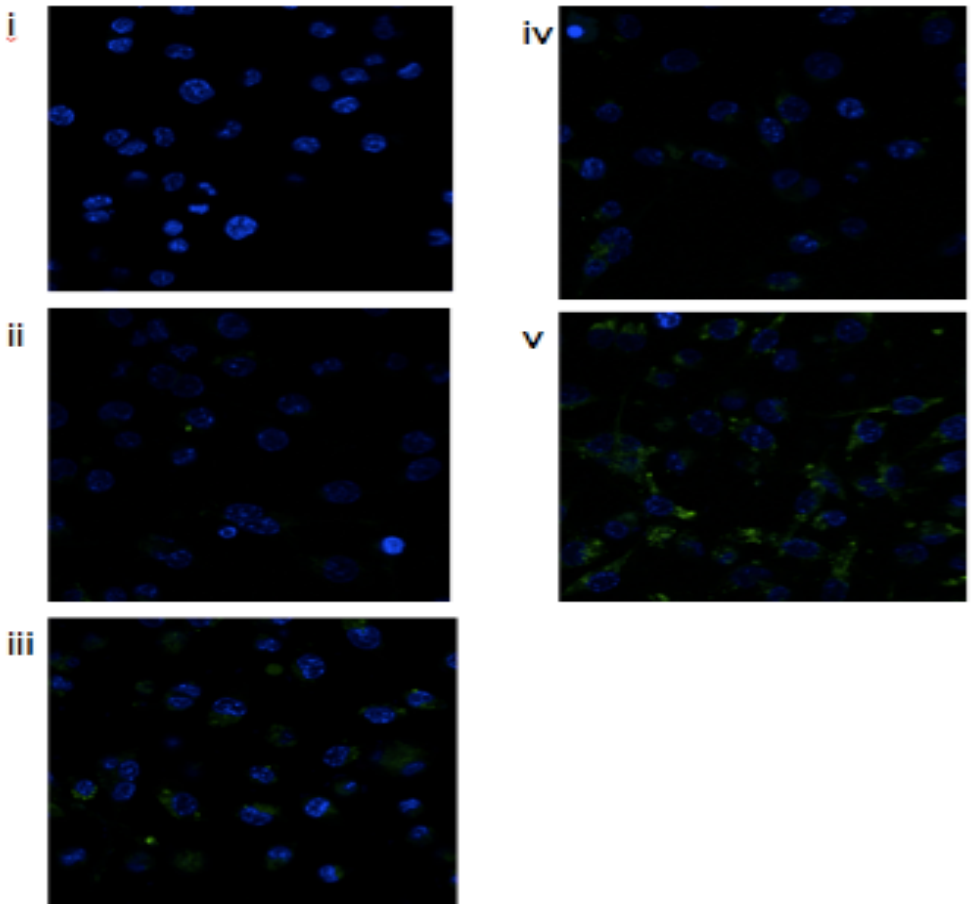
i
ii
iii
iv
v

Figure 5: Caspase-1 Activation in Murine Alveolar Macrophages post infection with *P.aeruginosa.* $4x10^5$ MH-S cells were plated in complete RPMI in 27mm Glass Base Dishes 24 hours prior to infection. Complete RPMI was washed once with serum free/ antibiotic free media 6 hours prior to infection. Overnight cultures of PA were diluted 1:50 and grown for 4 hours until mid-log phase (0.8 OD/600nm). MH-S cells were infected at a MOI of 50 and incubated at 37^oC, 5% CO_2 for 1 hour. Caspase probe (Invitrogen) was attached for 1 hour before fixing cells and viewing on a Zeiss Laser Scanning Microscope (LSM710). (A) Quantification of percentage of caspase-1^+ cells following infection with indicated PA strain. (B) MH-S were uninfected (i), infected with FRD1 (ii), FRD1131 (iii), PDO300 (iv), or WT PAO1 (v). Cells were stained for cleaved caspase-1 (FAM-FLICA) and DNA (Hoechst 33342). Images were taken at 63x magnification. Minimum of 100 cells were counted for quantification. Data are sum of triplicate experiments. Statistical analysis was performed by ANOVA followed by Tukey's test. *P<0.05, **P<0.01, ***P<0.001, ****P<0.0001, ns: not significant.

A.

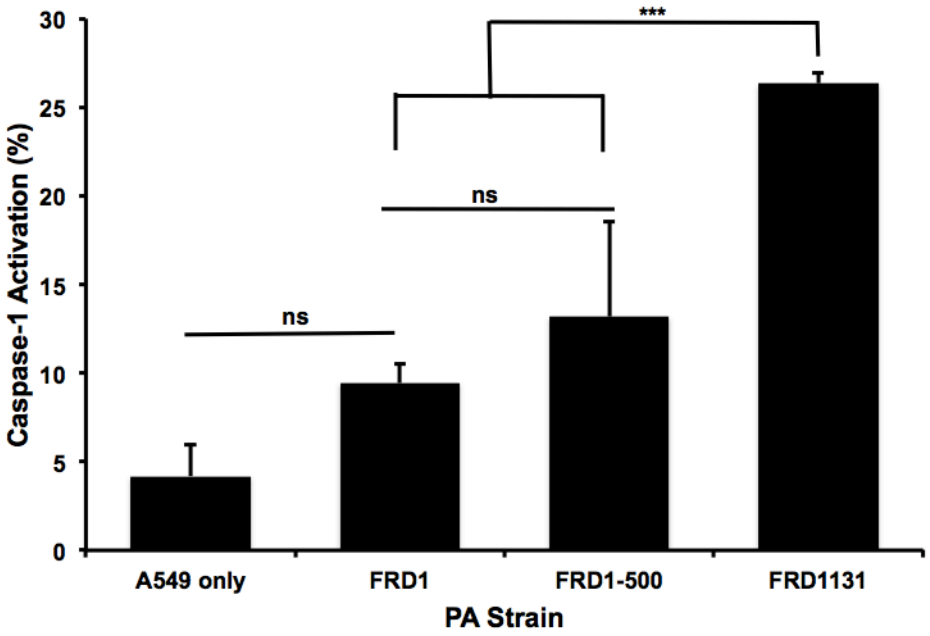
30
25
20
15
10
5
0
Caspase-1 Activation (%)
***
ns
ns
A549 only
FRD1
FRD1-500
FRD1131
PA Strain

B.

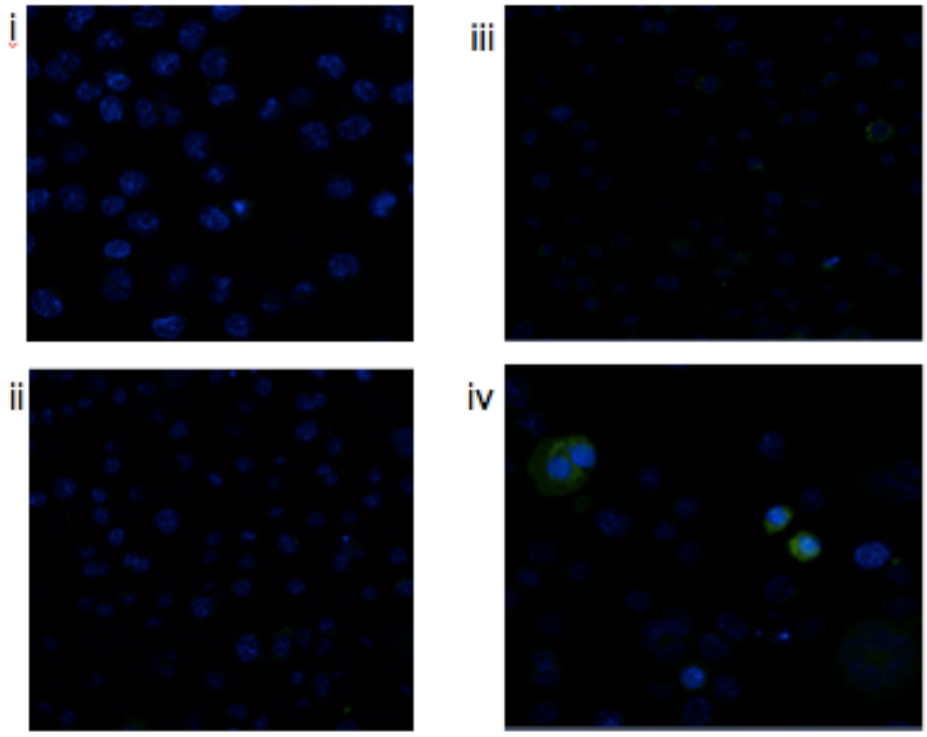
i
iii
ii
iv

Figure 6: Caspase-1 Activation in A549 epithelial cells post infection with varying *P. aeruginosa* at various MOI. $4x10^5$ A549 cells were plated in complete F12-HAMS in 27mm Glass Base Dishes 24 hours prior to infection. Complete F-12 HAMS was washed once with serum free/ antibiotic free media 6 hours prior to infection. Overnight cultures of PA were diluted 1:50 and grown for 4 hours until mid-log phase (0.8 OD/600nm). A549 cells were infected at a MOI of 50 and incubated at 37^oC, 5% CO_2 for 1 hour. Caspase probe (Invitrogen) was attached for 1 hour before fixing cells and viewing on a Zeiss Laser Scanning Microscope (LSM710). (A) Quantification of percentage of caspase-1^+ cells following infection with indicated PA strain. (B) A549 cells were uninfected (i), infected with FRD1 (ii), FRD1-MOI 500 (iii), or FRD1131 (iv). Cells were stained for cleaved caspase-1 (FAM-FLICA) and DNA (Hoechst 33342). Images were taken at 63x magnification. Minimum of 100 cells were counted for quantification. Data are sum of triplicate experiments. Statistical analysis was performed by ANOVA followed by Tukey's test. *P<0.05, **P<0.01, ***P<0.001, ****P<0.0001, ns: not significant.

A.

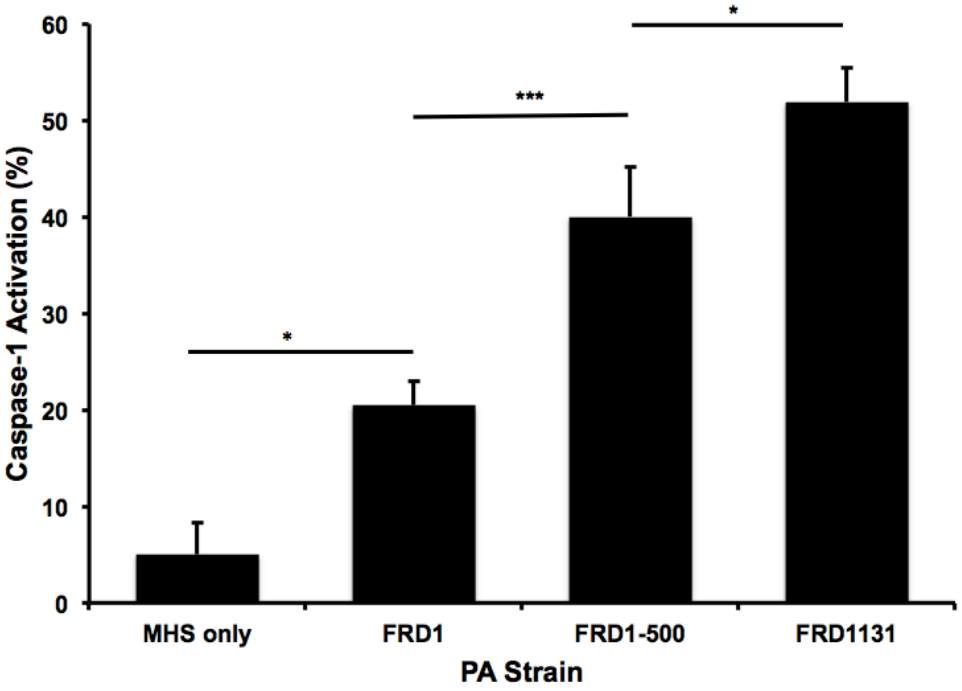
60
50
40
30
20
10
0
Caspase-1 Activation (%)
*
***
*
MHS only
FRD1
FRD1-500
FRD1131
PA Strain

B.

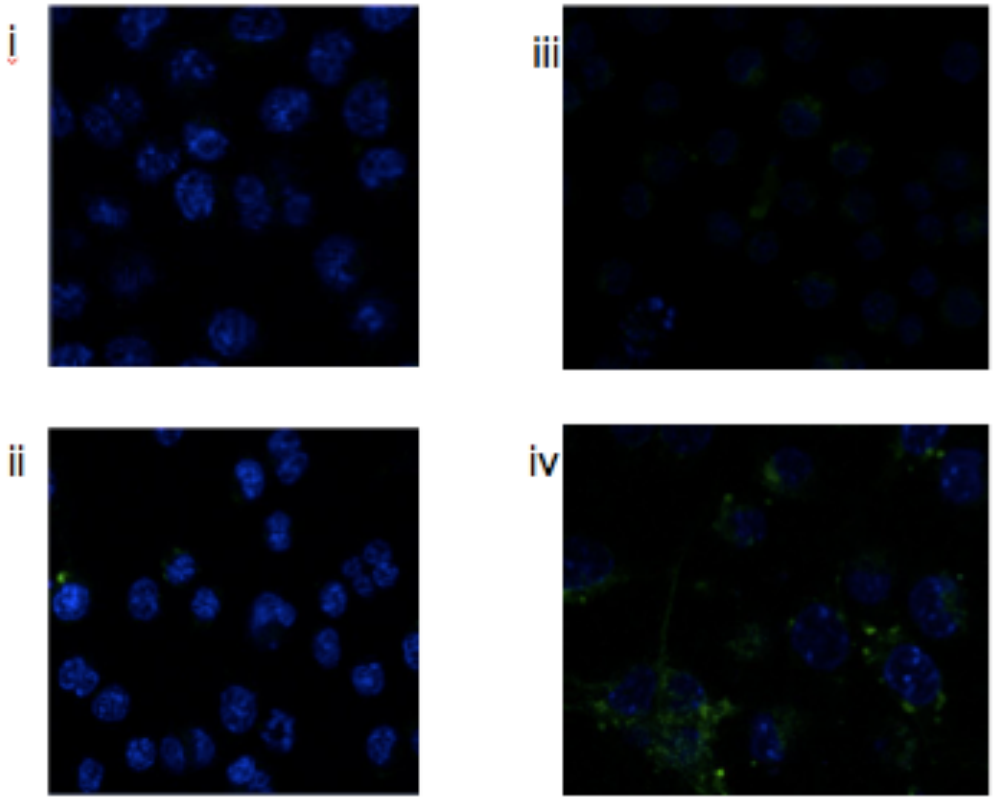
i
iii
ii
iv

Figure 7: Caspase-1 Activation in Murine Alveolar Macrophages post infection with *P. aeruginosa* at various MOI. $4x10^5$ MH-S cells were plated in complete RPMI in 27mm Glass Base Dishes 24 hours prior to infection. Complete RPMI was washed once with serum free/ antibiotic free media 6 hours prior to infection. Overnight cultures of PA were diluted 1:50 and grown for 4 hours until mid-log phase (0.8 OD/600nm). MH-S cells were infected at a MOI of 50 and incubated at 37^oC, 5% CO_2 for 1 hour. Caspase probe (Invitrogen) was attached for 1 hour before fixing cells and viewing on a Zeiss Laser Scanning Microscope (LSM710). (A) Quantification of percentage of caspase-1^+ cells following infection with indicated PA strain. (B) MH-S were uninfected (i), infected with FRD1 (ii), FRD1-MOI 500 (iii), or FRD1131 (iv). Cells were stained for cleaved caspase-1 (FAM-FLICA) and DNA (Hoechst 33342). Images were taken at 63x magnification. Minimum of 100 cells were counted for quantification. Data are sum of triplicate experiments. Statistical analysis was performed by ANOVA followed by Tukey's test. *P<0.05, **P<0.01, ***P<0.001, ****P<0.0001, ns: not significant

A.

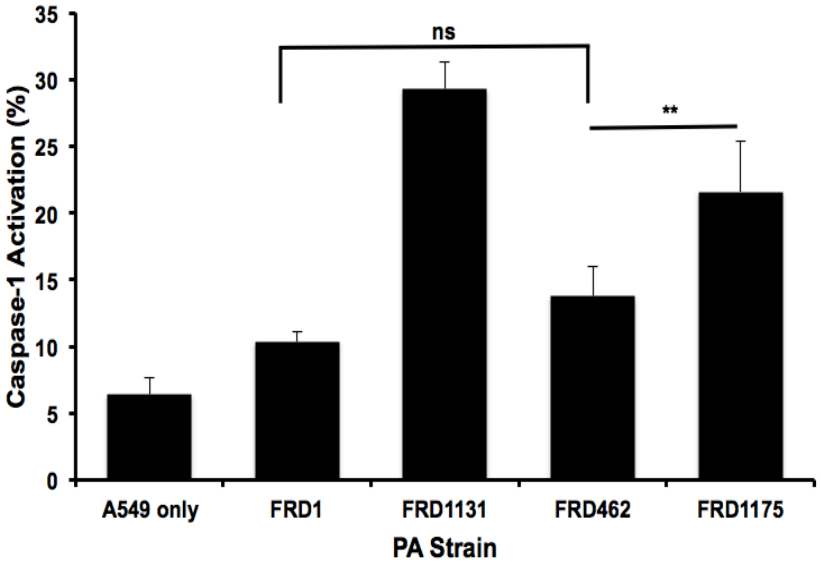
Caspase-1 Activation (%)
35
30
25
20
15
10
5
0
ns
**
A549 only
FRD1
FRD1131
FRD462
FRD1175
PA Strain

B.

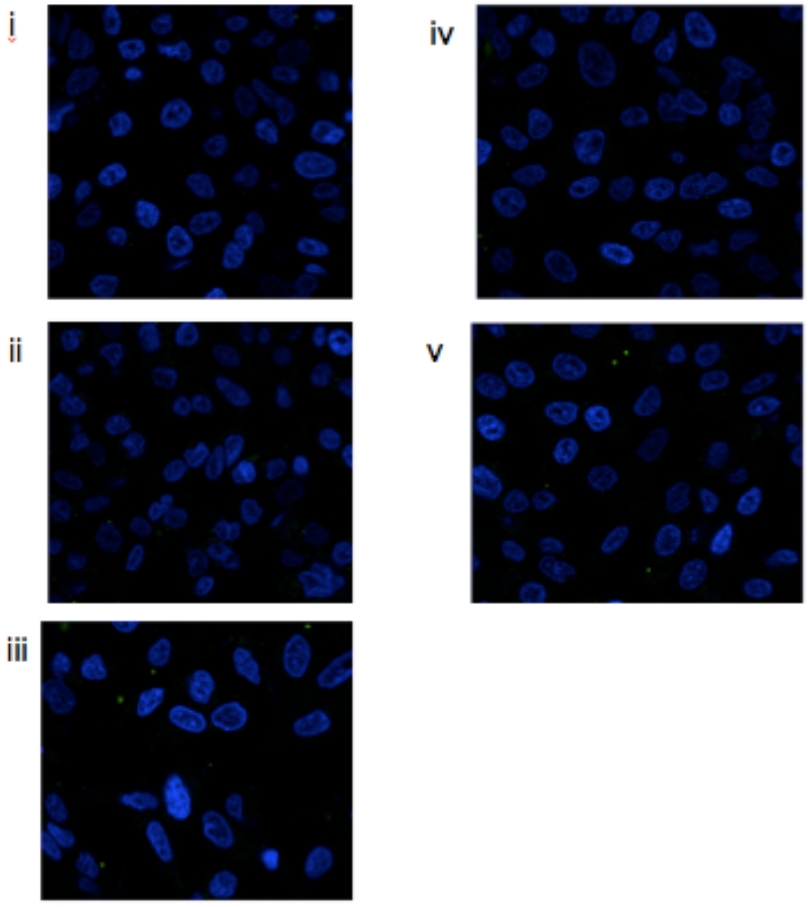
i
ii
iii
iv
v

Figure 8: Caspase-1 Activation in A549 epithelial cells post infection with *P. aeruginosa* alginate structural mutants. . $4x10^5$ A549 cells were plated in complete F12-HAMS in 27mm Glass Base Dishes 24 hours prior to infection. Complete F-12 HAMS was washed once with serum free/ antibiotic free media 6 hours prior to infection. Overnight cultures of PA were diluted 1:50 and grown for 4 hours until mid-log phase (0.8 OD/600nm). A549 cells were infected at a MOI of 50 and incubated at 37^oC, 5% CO_2 for 1 hour. Caspase probe (Invitrogen) was attached for 1 hour before fixing cells and viewing on a Zeiss Laser Scanning Microscope (LSM710). (A) Quantification of percentage of caspase-1^+ cells following infection with indicated PA strain. (B) A549 cells were uninfected (i), infected with FRD1 (ii), FRD1131 (iii), FRD462 (iv), or FRD1175 (v). Cells were stained for cleaved caspase-1 (FAM-FLICA) and DNA (Hoechst 33342). Images were taken at 63x magnification. Minimum of 100 cells were counted for quantification. Data are sum of triplicate experiments. Statistical analysis was performed by ANOVA followed by Tukey's test. *P<0.05, **P<0.01, ***P<0.001, ****P<0.0001, ns: not significant.

A.

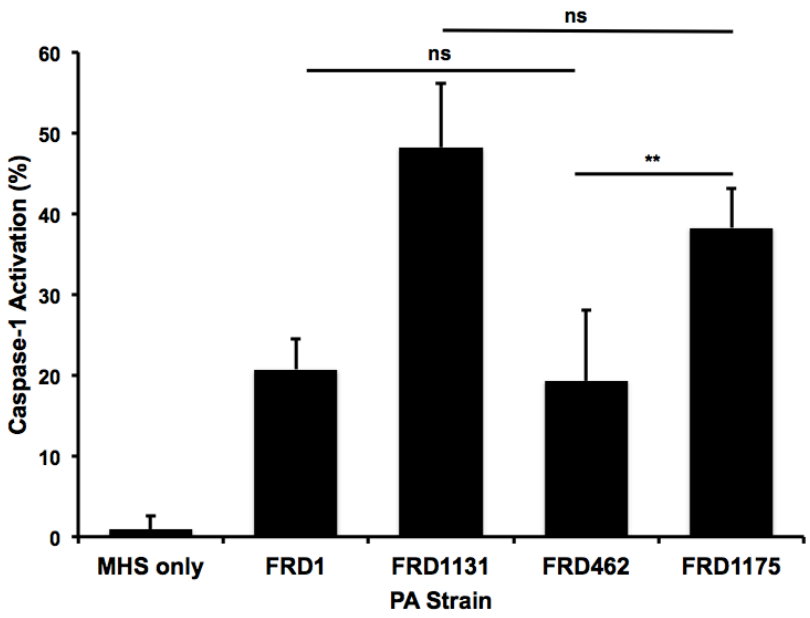
ns
ns
**
60
50
40
30
20
10
0
Caspase-1 Activation (%)
MHS only
FRD1
FRD1131
FRD462
FRD1175
PA Strain

B.

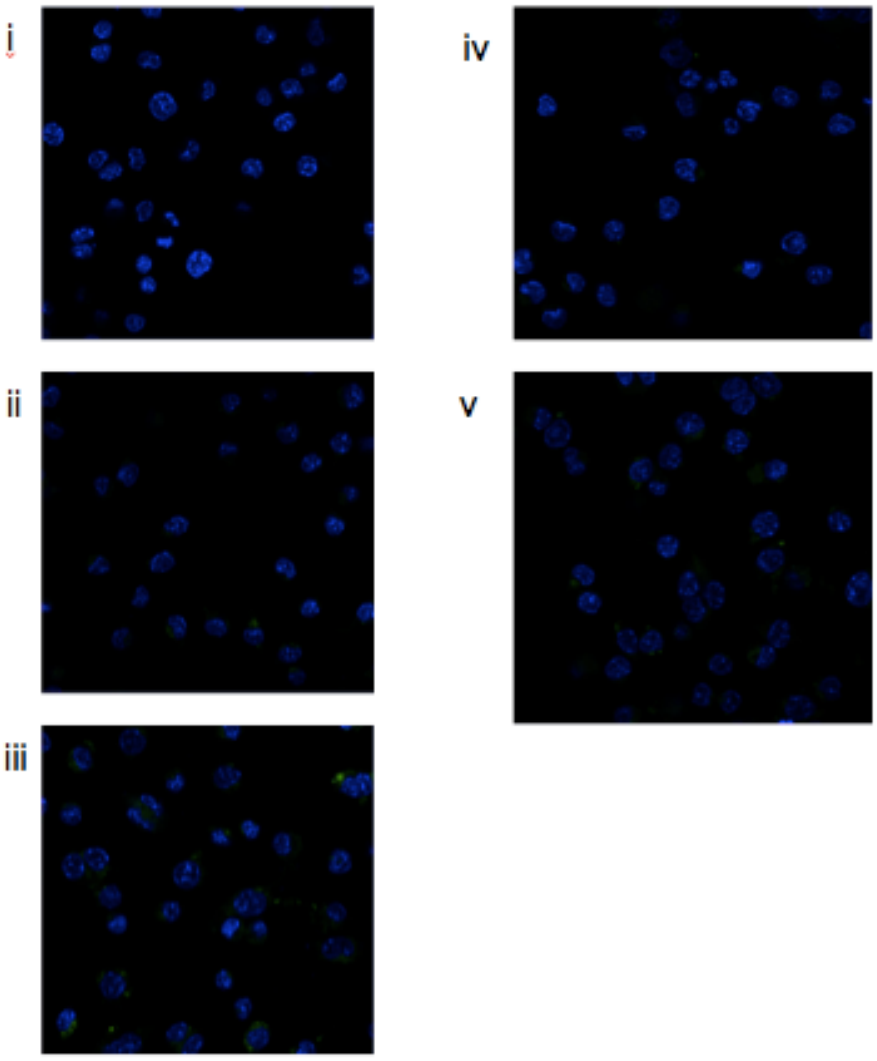
i
ii
iii
iv
v

Figure 9: Caspase-1 Activation in Murine Alveolar Macrophages post infection with *P. aeruginosa* alginate structural mutants. $4x10^5$ MH-S cells were plated in complete RPMI in 27mm Glass Base Dishes 24 hours prior to infection. Complete RPMI was washed once with serum free/ antibiotic free media 6 hours prior to infection. Overnight cultures of PA were diluted 1:50 and grown for 4 hours until mid-log phase (0.8 OD/600nm). MH-S cells were infected at a MOI of 50 and incubated at 37^oC, 5% CO_2 for 1 hour. Caspase probe (Invitrogen) was attached for 1 hour before fixing cells and viewing on a Zeiss Laser Scanning Microscope (LSM710). (A) Quantification of percentage of caspase-1^+ cells following infection with indicated PA strain. (B) MH-S were uninfected (i), infected with FRD1 (ii), FRD1131 (iii), FRD462 (iv), or FRD1175 (v). Cells were stained for cleaved caspase-1 (FAM-FLICA) and DNA (Hoechst 33342). Images were taken at 63x magnification. Minimum of 100 cells were counted for quantification. Data are sum of triplicate experiments. Statistical analysis was performed by ANOVA followed by Tukey's test. *P<0.05, **P<0.01, ***P<0.001, ****P<0.0001, ns: not significant

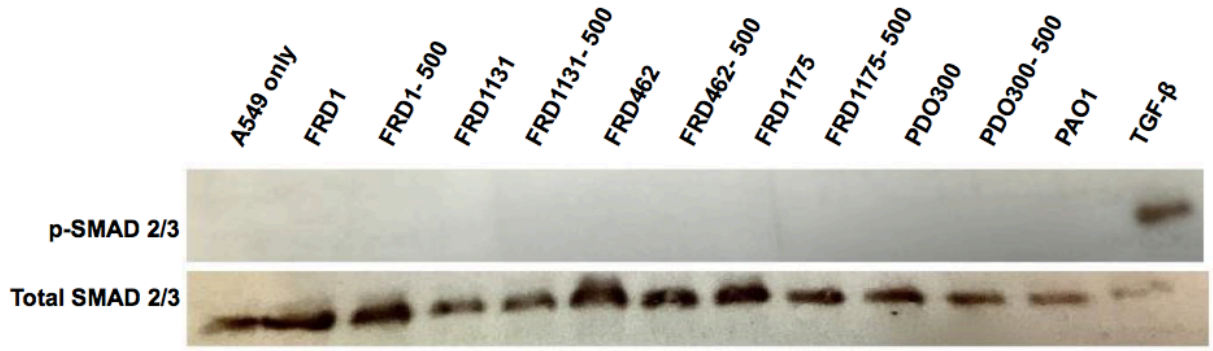

Figure 10: Western Analysis of TGF-β activation in A549 epithelial cells. 2x10^5 A549 cells were plated in F-12 HAMS in 6 well plates 24 hours prior to infection. Overnight cultures of *Pseudomonas aeruginosa* were diluted 1:50 and grown for 4 hours until mid-log phase (0.8 OD/600nm). A549 cells were infected at a MOI of 50:1 or 500:1 and incubated at 37^{o}C, 5% CO_2 for 1 hour. Lysates were separated on 10% polyacrylamide gel and exposed to film.

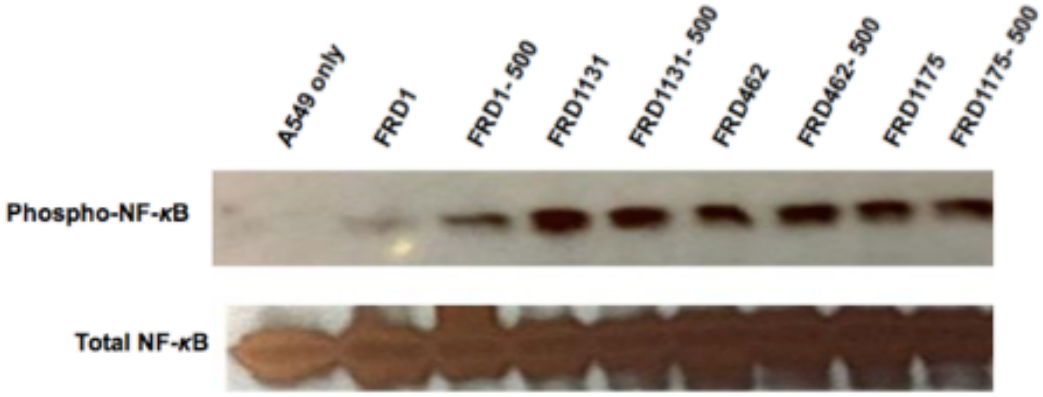

Figure 11: Western Analysis of NF-κB activation in A549 epithelial cells. 2x10^5 A549 cells were plated in F-12 HAMS in 6 well plates 24 hours prior to infection. Overnight cultures of *Pseudomonas aeruginosa* were diluted 1:50 and grown for 4 hours until mid-log phase (0.8 OD/600nm). A549 or MH-S cells were infected at a MOI of 50:1 or 500:1 and incubated at 37^{o}C, 5% CO_2 for 1 hour. Lysates were separated on 10% polyacrylamide gel and exposed to film.

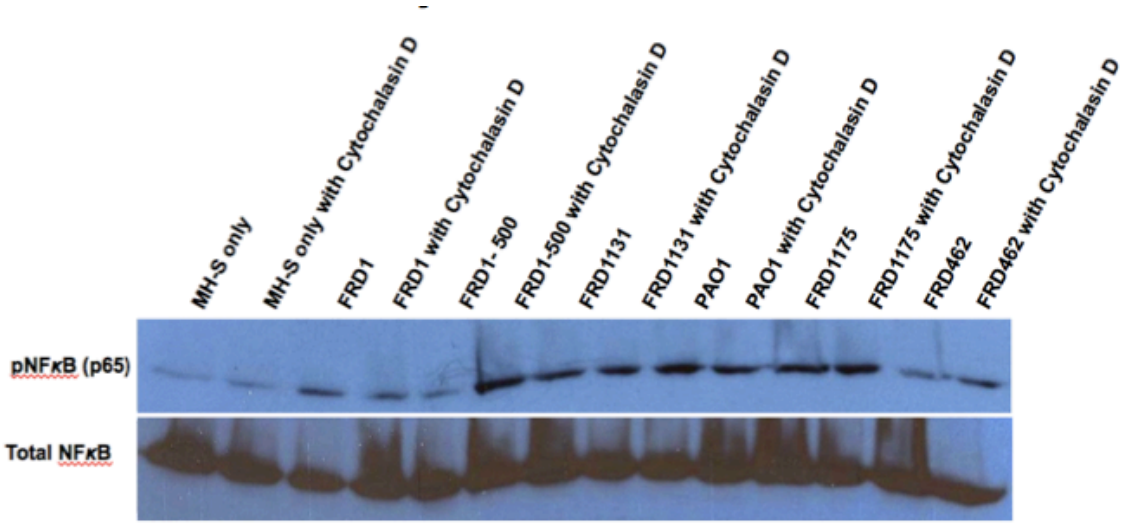

Figure 12: Western Analysis of NF-κB activation in Murine Alveolar Macrophages. 2x10^5 MHS cells were plated in RPMI in 6 well plates 24 hours prior to infection. Overnight cultures of *Pseudomonas aeruginosa* were diluted 1:50 and grown for 4 hours until mid-log phase (0.8 OD/600nm). MH-S cells were infected at a MOI of 50:1 or 500:1 and incubated at 37^{o}C, 5% CO_2 for 1 hour. Lysates were separated on 10% polyacrylamide gel and exposed to film.

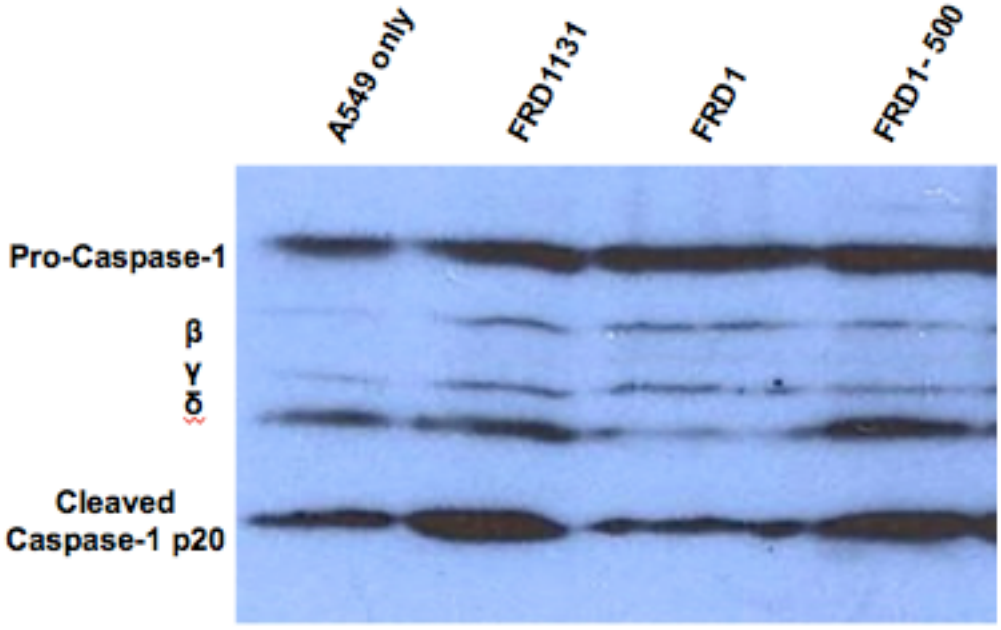

Figure 13: Western Analysis of Caspase-1 in A549 epithelial cells. 2x10^5 A549 cells were plated in F-12 HAMS in 6 well plates 24 hours prior to infection. Overnight cultures of *Pseudomonas aeruginosa* were diluted 1:50 and grown for 4 hours until mid-log phase (0.8 OD/600nm). A549 cells were infected at a MOI of 50:1 or 500:1 and incubated at 37^{o}C, 5% CO_2 for 1 hour. Lysates were separated on 12% polyacrylamide gel and exposed to film.

List of References

1. Berger, M., *Lung inflammation early in cystic fibrosis: bugs are indicted, but the defense is guilty.* Am J Respir Crit Care Med, 2002. **165**(7): p. 857-8.
2. Biwersi, J., N. Emans, and A.S. Verkman, *Cystic fibrosis transmembrane conductance regulator activation stimulates endosome fusion in vivo.* Proc Natl Acad Sci U S A, 1996. **93**(22): p. 12484-9.
3. Casadevall, A. and L.A. Pirofski, *Host-pathogen interactions: basic concepts of microbial commensalism, colonization, infection, and disease.* Infect Immun, 2000. **68**(12): p. 6511-8.
4. Chitnis, C.E. and D.E. Ohman, *Genetic analysis of the alginate biosynthetic gene cluster of Pseudomonas aeruginosa shows evidence of an operonic structure.* Mol Microbiol, 1993. **8**(3): p. 583-93.
5. Cobb, L.M., et al., *Pseudomonas aeruginosa flagellin and alginate elicit very distinct gene expression patterns in airway epithelial cells: implications for cystic fibrosis disease.* J Immunol, 2004. **173**(9): p. 5659-70.
6. Davies, J.C., *Pseudomonas aeruginosa in cystic fibrosis: pathogenesis and persistence.* Paediatr Respir Rev, 2002. **3**(2): p. 128-34.
7. Denes, A., G. Lopez-Castejon, and D. Brough, *Caspase-1: is IL-1 just the tip of the ICEberg?* Cell Death Dis, 2012. **3**: p. e338.

8. Donaldson, S.H. and R.C. Boucher, *Update on pathogenesis of cystic fibrosis lung disease.* Curr Opin Pulm Med, 2003. **9**(6): p. 486-91.

9. Eckrich, J., et al., *Airway inflammation in mild cystic fibrosis.* J Cyst Fibros, 2016.

10. Eddens, T. and J.K. Kolls, *Host defenses against bacterial lower respiratory tract infection.* Curr Opin Immunol, 2012. **24**(4): p. 424-30.

11. Fakhr, M.K., et al., *Regulation of alginate biosynthesis in Pseudomonas syringae pv. syringae.* J Bacteriol, 1999. **181**(11): p. 3478-85.

12. Fleckenstein, J.M. and D.J. Kopecko, *Breaching the mucosal barrier by stealth: an emerging pathogenic mechanism for enteroadherent bacterial pathogens.* J Clin Invest, 2001. **107**(1): p. 27-30.

13. Franklin, M.J. and D.E. Ohman, *Identification of algI and algJ in the Pseudomonas aeruginosa alginate biosynthetic gene cluster which are required for alginate O acetylation.* J Bacteriol, 1996. **178**(8): p. 2186-95.

14. Gellatly, S.L. and R.E. Hancock, *Pseudomonas aeruginosa: new insights into pathogenesis and host defenses.* Pathog Dis, 2013. **67**(3): p. 159-73.

15. Hagemann, T., F. Balkwill, and T. Lawrence, *Inflammation and cancer: a double-edged sword.* Cancer Cell, 2007. **12**(4): p. 300-1.

16. Hara, H., et al., *Phosphorylation of the adaptor ASC acts as a molecular switch that controls the formation of speck-like aggregates and inflammasome activity.* Nat Immunol, 2013. **14**(12): p. 1247-55.

17. Hauser, A.R., *The type III secretion system of Pseudomonas aeruginosa: infection by injection.* Nat Rev Microbiol, 2009. **7**(9): p. 654-65.

18. Hawdon, N.A., et al., *Cellular responses of A549 alveolar epithelial cells to serially collected Pseudomonas aeruginosa from cystic fibrosis patients at different stages of pulmonary infection.* FEMS Immunol Med Microbiol, 2010. **59**(2): p. 207-20.

19. Heijerman, H., *Infection and inflammation in cystic fibrosis: a short review.* J Cyst Fibros, 2005. **4 Suppl 2**: p. 3-5.

20. Hogardt, M. and J. Heesemann, *Adaptation of Pseudomonas aeruginosa during persistence in the cystic fibrosis lung.* Int J Med Microbiol, 2010. **300**(8): p. 557-62.

21. Hoiby, N., B. Frederiksen, and T. Pressler, *Eradication of early Pseudomonas aeruginosa infection.* J Cyst Fibros, 2005. **4 Suppl 2**: p. 49-54.

22. Horsman, S.R., R.A. Moore, and S. Lewenza, *Calcium chelation by alginate activates the type III secretion system in mucoid Pseudomonas aeruginosa biofilms.* PLoS One, 2012. **7**(10): p. e46826.

23. Huang, F.C., *The differential effects of 1,25-dihydroxyvitamin D3 on Salmonella-induced interleukin-8 and human beta-defensin-2 in intestinal epithelial cells.* Clin Exp Immunol, 2016. **185**(1): p. 98-106.

24. Janeway, C.A., Jr. and R. Medzhitov, *Innate immune recognition.* Annu Rev Immunol, 2002. **20**: p. 197-216.

25. Kipnis, E., T. Sawa, and J. Wiener-Kronish, *Targeting mechanisms of Pseudomonas aeruginosa pathogenesis.* Med Mal Infect, 2006. **36**(2): p. 78-91.

26. Klockgether, J., et al., *Genome diversity of Pseudomonas aeruginosa PAO1 laboratory strains.* J Bacteriol, 2010. **192**(4): p. 1113-21.

27. Lawrence, T., *The nuclear factor NF-kappaB pathway in inflammation.* Cold Spring Harb Perspect Biol, 2009. **1**(6): p. a001651.

28. Leid, J.G., et al., *The exopolysaccharide alginate protects Pseudomonas aeruginosa biofilm bacteria from IFN-gamma-mediated macrophage killing.* J Immunol, 2005. **175**(11): p. 7512-8.

29. Lopez-Castejon, G. and D. Brough, *Understanding the mechanism of IL-1beta secretion.* Cytokine Growth Factor Rev, 2011. **22**(4): p. 189-95.

30. Lynn, D.J., et al., *Curating the innate immunity interactome.* BMC Syst Biol, 2010. **4**: p. 117.

31. Magnan, A., et al., *Transforming growth factor beta in normal human lung: preferential location in bronchial epithelial cells.* Thorax, 1994. **49**(8): p. 789-92.

32. Medzhitov, R. and C.A. Janeway, Jr., *Innate immunity: the virtues of a nonclonal system of recognition.* Cell, 1997. **91**(3): p. 295-8.

33. Miao, E.A., et al., *Innate immune detection of the type III secretion apparatus through the NLRC4 inflammasome.* Proc Natl Acad Sci U S A, 2010. **107**(7): p. 3076-80.

34. Moreau-Marquis, S., B.A. Stanton, and G.A. O'Toole, *Pseudomonas aeruginosa biofilm formation in the cystic fibrosis airway.* Pulm Pharmacol Ther, 2008. **21**(4): p. 595-9.

35. Muir, A., et al., *Toll-like receptors in normal and cystic fibrosis airway epithelial cells.* Am J Respir Cell Mol Biol, 2004. **30**(6): p. 777-83.

36. Ohman, D.E., *Molecular genetics of exopolysaccharide production by mucoid Pseudomonas aeruginosa.* Eur J Clin Microbiol, 1986. **5**(1): p. 6-10.

37. Patankar, Y.R., et al., *Flagellar motility is a key determinant of the magnitude of the inflammasome response to Pseudomonas aeruginosa.* Infect Immun, 2013. **81**(6): p. 2043-52.

38. Pier, G.B., et al., *Role of alginate O acetylation in resistance of mucoid Pseudomonas aeruginosa to opsonic phagocytosis.* Infect Immun, 2001. **69**(3): p. 1895-901.

39. Rommens, J.M., et al., *Identification of the cystic fibrosis gene: chromosome walking and jumping.* Science, 1989. **245**(4922): p. 1059-65.

40. Rowe III, W., *The Role of Alginate in the Inhibition of Macrophage Phagocytosis.* VCU Theses and Disertations, 2013.

41. Tart, A.H., M.C. Wolfgang, and D.J. Wozniak, *The alternative sigma factor AlgT represses Pseudomonas aeruginosa flagellum biosynthesis by inhibiting expression of fleQ.* J Bacteriol, 2005. **187**(23): p. 7955-62.

42. Vance, R.E., *The NAIP/NLRC4 inflammasomes.* Curr Opin Immunol, 2015. **32**: p. 84-9.

43. Welsh, M.J. and A.E. Smith, *Molecular mechanisms of CFTR chloride channel dysfunction in cystic fibrosis.* Cell, 1993. **73**(7): p. 1251-4.

44. Wolfram, F., et al., *Catalytic mechanism and mode of action of the periplasmic alginate epimerase AlgG.* J Biol Chem, 2014. **289**(9): p. 6006-19.

45. Wood, L.F. and D.E. Ohman, *Cell wall stress activates expression of a novel stress response facilitator (SrfA) under sigma22 (AlgT/U) control in Pseudomonas aeruginosa.* Microbiology, 2015. **161**(Pt 1): p. 30-40.

46. Wu, W., et al., *MucA-mediated coordination of type III secretion and alginate synthesis in Pseudomonas aeruginosa.* J Bacteriol, 2004. **186**(22): p. 7575-85.

Vita

Brian Edward Crossley was born on October 29, 1991 in Albany, NY and is an American citizen. He graduated from Monacan High School in Richmond, VA in 2010. He received a Bachelor of Science degree in Biology from Virginia Commonwealth University in 2014. He began pursuit of a Master of Science degree in August 2014.